Effect of annealing on the structural and optical properties of In_2S_3 films

A.E. Bekheet*[1,2], E.H.El-Khawas[3]
1.Physics Department, Faculty of Education, Ain Shams University, Cairo, Egypt
2. Physics Department, Faculty of Science, University of Tabuk, KSA.
3. Higher Technological Institute, El-Ascher Men Ramadan City, Egypt.

Abstract

In_2S_3 thin films were prepared by thermal evaporation technique on glass substrates. X-ray diffraction analysis for the as-deposited films showed that they have amorphous structure. On annealing at 573 K films have β- phase tetragonal polycrystalline structure. The optical constants n and k of the as-deposited and annealed films have been calculated from optical transmittance and reflectance data in the wavelength range 350–2500 nm using Murmann's exact equations. Both n and k are practically independent on the film thickness in the range 210–470 nm. The optical transitions are found to be allowed indirect and direct for the as-deposited and annealed films, and the corresponding energy gaps increase with increasing annealing temperature.

Keywords:

* E-mail: ashraf_bekheet@hotmail.com, telephone no. 00966507072025

1. INTRODUCTION.

Studies of $A^{III}_2B^{VI}_3$ compounds with A = Ga, In, Tl and B= S, Se, Te, have attracted the attention of researchers because of their importance as good photovoltaic materials. Moreover, these compounds have attractive properties for applications in electro-thermal devices [1] such as solid solution electrodes. These compounds have mainly zinc-blende and wurtzite structures with tetrahedral bonding[1]. These are the simplest types of defective structures in which some of the crystallographically equivalent sites are only partially occupied and that the lattice has vacant sites[2]. The presence of a large number of defects destroyed the periodicity of the lattice and distorts the crystal field. Therefore, the semiconducting properties of these materials should be strongly affected by annealing which increases the degree of ordering and hence their physical properties [1]. Several papers have been published to investigate their structure, electrical and optical properties and they confirmed that these properties have been affected by annealing [3-10].

In_2S_3 is a member of the above family and is a promising candidate for optoelectronic and photovoltaic applications [11-14]. It has very interesting physical properties due to its stability, wide band gap and photoconductive behavior [15]. It can be used as a buffer layer for photovoltaic applications[16]. It can be used as an effective nontoxic substitute for cadmium sulfide (CdS) in Copper Indium Gallium Selenide (CIGS) based solar cells [14,17]. The motivation behind this is not only to eliminate toxic cadmium, but also to improve light transmission in the blue wavelength region by using a material having band gap wider than that of cadmium sulfide (CdS). CIGS based solar cell, with In_2S_3 as the buffer layer, could reach efficiencies (16.4%) near to those obtained by devices made with standard CdS buffer layer [17].

The optical properties of In_2S_3 thin films were studied by several authors [11,16,18-25]. Because of the difficulty in preparing stoichiometric In_2S_3 thin films regardless of the utilizing method, the structure and the value of the fundamental absorption edge shows differences among the published data.

In this paper, the optical properties of In_2S_3 thin films, deduced from optical transmittance and reflectance in the spectral range of 350 - 2500 nm were studied. The obtained data are analyzed using accurate method to determine the optical constants (refractive index n, absorption index k and absorption coefficient α). An analysis of the absorption coefficient has been carried out to obtain the optical band gap and determine the nature of the transitions involved. The effect of annealing at different temperatures of 423, 473, 523 and 573 K on the structure and optical properties are also studied. Our results are compared with those obtained previously.

2- EXPERIMENTAL PROCEDURE.

Films with different thicknesses (210 - 470 nm) of In_2S_3 were obtained onto glass substrates by thermal evaporation of bulk material under vacuum ($2x10^{-5}$ Pa). The substrate temperature was held at that of room during deposition

process. X-ray diffraction (XRD) analysis was used to investigate the structure of the obtained films. Their chemical composition was checked by energy dispersive X-ray (EDX) analysis using scanning electron microscope (Joel 5400).

The optical transmittance and reflectance of the film samples of different thickness deposited onto glass substrate was measured at room temperature using un-polarized light at normal incidence in the wavelength range (350–2500 nm) using a dual beam spectrophotometer ((JASCO model V-570 UV–VIS-NIR). Film thickness was calculated from the interference fringes of the transmittance spectrum to an accuracy of better than 1% [26]. The absolute values of transmittance T and reflectance R were calculated using the following equation[27-29]:

$$T = \left(\frac{I_{ft}}{I_g}\right)(1 - R_g) \quad \text{.....(1)}$$

where I_{ft} and I_g are the intensity of light transmitted through the film substrate system and the glass reference, respectively. R_g is the reflectance of glass substrate, and

$$R = ((I_{fr}/ I_m)R_m [1 + (1 - R_g)^2]) - T^2R_g \; ;\text{.....(2)}$$

where I_m is the intensity of light reflected from the reference mirror, I_{fr} is the intensity of light reflected from the sample reaching the detector and R_m the mirror reflectance.

The transmittance T(λ) and reflectance R(λ) can be expressed by Murmann's exact equations [30] as:

$$T = \frac{16\, n_o\, n_s\, (n^2 + k^2)}{E\, e^{\beta} + F\, e^{-\beta} + 2\, G \cos\gamma + 4\, H \sin\gamma} \quad (3)$$

$$R = \frac{A\, e^{\beta} + B\, e^{-\beta} + 2\, C \cos\gamma + 4\, D \cos\gamma}{E\, e^{\beta} + F\, e^{-\beta} + 2\, G \cos\gamma + 4\, H \sin\gamma} \quad (4)$$

where,

$$\gamma = 4\pi\, n \frac{d}{\lambda} \quad , \quad \beta = 4\pi\, k \frac{d}{\lambda}$$

$$A = [(n - n_o)^2]\; [(n + n_s)^2 + k^2],$$

$$B = [(n - n_s)^2 + k^2]\; [(n + n_s)^2 + k^2],$$

$$C = (n^2 + k^2)\; (n_0^2 - n_s^2) - (n^2 + k^2)^2 - n_0^2\, n_s^2 - 4\, n_s\, n_0\, k^2$$

$$D = k\,(n_s - n_o)\; (n + k^2 + n_s\, n_o),$$

$$E = [(n + n_o)^2 + k^2]\; [(n + n_s)^2 + k^2],$$

$$F = [(n - n_o)^2 + k^2]\; [(n + n_s)^2 + k^2],$$

$$G = (n^2 + k^2)\; (n_0^2 + n_s^2) - (n^2 + k^2)^2 - n_0^2\, n_s^2 + 4\, n_s\, n_0\, k^2,$$

and $$H = k\,(n_s + n_o)^2\; (n + k^2 - n_s\, n_o)$$

As n_0, n_s and n are the refractive indices of air, substrate and film respectively, k is the absorption index of film and d is the film thickness.

A computer based program was used in computation of R(n,k) and T(n,k) [31] which is basically a uni-variance search technique. First $|R(n,k)-R_{exp}|$ was minimized with respect to n, then $|T(n,k)-T_{exp}|$ was minimized with respect to k; this strategy is not a good one for general optimization problems, where R_{exp} and T_{exp} are the experimentally determined values of R and T respectively; R(n,k) and T(n,k) are the calculated values of R and T using Murmann's equations. [30].

The method is basically a bivariance search technique [31], by which the two values $(\Delta R)^2$ and $(\Delta T)^2$ are minimized simultaneously, where,

$$(\Delta R)^2 = |\, R(n,k)-R_{exp}\,|^2 = \min\text{..... (5)}$$

$$(\Delta T)^2 = |\, T(n,k)-T_{exp}\,|^2 = \min\text{.....(6)}$$

The research in this method was carried out through two operations, which are the bivariant search operation and step-length optimization operation.

In the first operation, ranges n_1 to n_2 and k_1 to k_2 are used to calculate R(n,k) and T(n,k) in each step. The variance $(\Delta R)^2$ and $(\Delta T)^2$ are calculated to obtain the minimum variance which converges to unique points and hence gives the optimum values of n and k simultaneously. The second operation was developed to speed up convergence (i.e. increase the runtime to improve the accuracy).

The values of n and k obtained at the minimum variance are noted as n_m and k_m. The values $[n_m-(n_2-n_1)/10]$ and $[k_m-(k_2-k_1)/10]$ are then compared to specific tolerance values (t_n=0.01) and (t_n=0.001), if these values are smaller than the tolerance values, then $n=n_m$ and $k=k_m$ and so the program will be terminated, otherwise the calculation will be repeated to obtain the equivalence.

The obtained films were annealed at different temperatures of 373, 423, 473, 523, and 573 K. The obtained films were annealed directly to the selected temperature for different periods of time, such that 0.25, 0.5, 1.0, 2.0 and 4 h until the intensity of transmitted light through the specimen became steady thus indicating the stability of the structure of the film under test. The optical transmittance and reflectance of the annealed films in the same spectral range were also measured.

3- RESULTS AND DISCUSSION.

3-1 STRUCTURAL IDENTIFICATION

X-ray diffraction patterns obtained for In_2S_3 in powder form illustrated that, it has polycrystalline nature of as shown in figure (1a). The result of indexing the pattern of the polycrystalline sample is found to be quite consistent with JCPDS card no. 73-1366 for tetragonal In_2S_3.

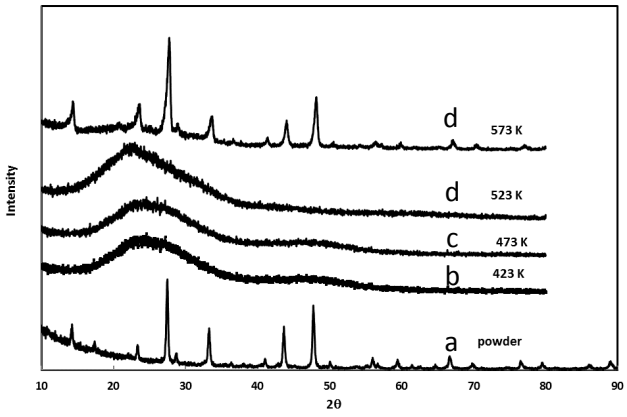

Fig.(1) X-ray diffraction of In_2S_3 powder and films annealed at different temperatures.

X-ray diffraction patterns were carried out for as-deposited In_2S_3 films of different thicknesses. Fig. (1b) illustrates one of these samples, which indicates that as-deposited In_2S_3 films have amorphous structure. The amorphous structure of the as-deposited films when the substrate is kept at room temperature is expected because the evaporating molecules precipitate randomly on its surface of the substrate and all the following condensed molecules also adhere randomly leading to disordered films of increased thickness. The loss of adequate kinetic energy for the precipitated molecule keeps them unable to orient themselves to produce the chain structure required for the crystalline structure of In_2S_3: The internal stresses generated in the layers of the film due to the continuous deposition of the hot molecule on the cold predeposited layers increase both the disorder and the degree of randomness which in turn leads to amorphous films whatever is their thickness when formed at room temperature.

To investigate the effect of annealing temperature on the structure of In_2S_3 films, samples of different thicknesses were annealed for 3 h at 423, 473, 523, and 573 K: As a representative example, X-ray diffraction patterns of annealed film of thickness 470 nm with that of the as-deposited are shown in Fig. 1a–e. It is clear that In_2S_3 films annealed at temperatures less than or equal to 523 K still have amorphous structure, while those annealed at 573 K have polycrystalline structure. The result of indexing the pattern of the polycrystalline sample is found to be also consistent with JCPDS card no. 73-1366 for tetragonal In_2S_3.

The effect of crystal size on the diffraction pattern is one of the phenomenon connected with optical gratings. The position of the maximum diffraction depends only on the groove spacing, but the width of the line decreases with increasing the number of the grooves[32]. Fig.(2a,b) shows the intensities for the broadened higher intensity (109) peak profile for the powder and the annealed film at 573 K. The crystallite size was evaluated using Sherrer equation [33]. The obtained values are 4.0785Å and 2.8561 Å for powder and annealed film respectively. This behavior of the crystallite size has its effects on the film hardness and ordering in structure.

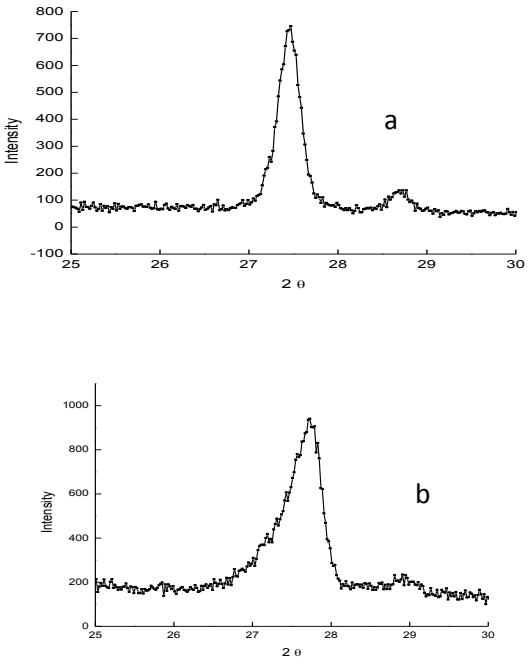

Fig.(2) The intensities for the broadened higher intensity (109) peak profile for :
a) powder and b) annealed film at 573 K.

3-2 DETERMINATION OF OPTICAL CONSTANTS

Fig.(3) shows the spectral distribution of transmittance (T) and reflectance (R) in the spectral range (350-2500 nm) for as-deposited In_2S_3 films of different thicknesses. It is indicated that at longer wavelengths T+R equals 1 indicating that films are transparent in these ranges and no light is absorbed.

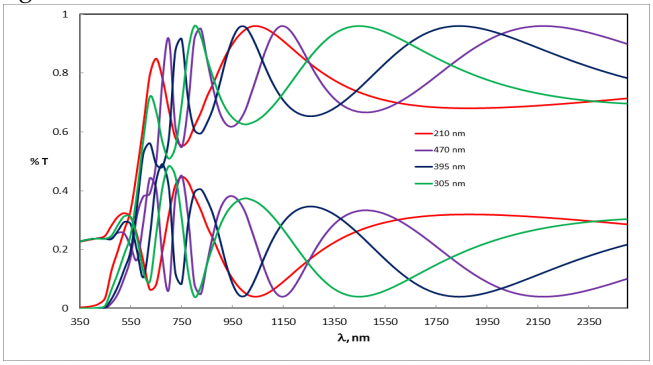

Fig.(3) The spectral distribution of transmittance (T) and reflectance (R) for as-deposited In_2S_3 films of different thicknesses.

The optical constants (refractive index n and the absorption index k) were_calculated in the spectral range (400-2500 nm) using Murmann's exact equations [30] via the technique described in above. By applying such a technique , unique values of n and k at any wavelength (λ) are obtained within the desired accuracy.

Fig (4) shows the spectral distribution of the refractive index (n) and absorption index (k) for the as – deposited In_2S_3 films. The maximum scatter between the data of the films of different thicknesses lies within the range of experimental error; accordingly both n and k are independent of the film thickness in the investigated range. There is an anomalous dispersion in the wavelength below 1200 nm and normal dispersion in the wavelength above 1200 nm.

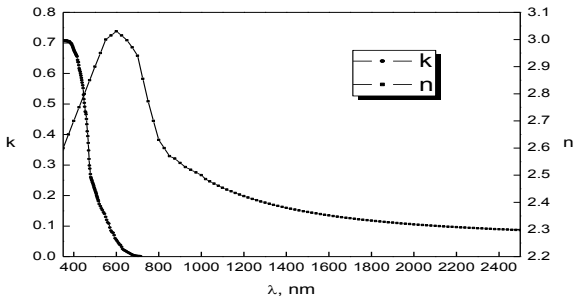

Fig.(4) The spectral distribution of reflective index n and absorption index (k) for as-deposited In_2S_3 films.

3.3 Optical energy gap determination:

The absorption coefficient (⍟) of as-deposited In_2S_3 films is **calculated** using the well-known equation $\alpha = 4\pi k/\lambda$ in which k is substituted by its mean value obtained from Fig.(4). The dependence of the absorption coefficient, α, on the photon energy, hν, is important to obtain information about direct or indirect inter-band transitions.

The variation in absorption coefficient with photon energy for band-to-band transitions is obtained using:

$$\alpha h\nu = A\,(h\nu - E_g)^{1/r} \qquad (7)$$

where A is constant, E_g is the optical energy gap, and r determines the type of transitions, which is equal 2 and 1/2 in case of allowed direct and indirect transitions and is equal 1/3 and 2/3 in case of forbidden direct and indirect optical transitions. The dependence of $(\alpha h\nu)^{1/r}$ and photon energy (hν) for onset gaps was discussed and plotted for different values of r.

Fig. (5) shows that plots of $(\alpha h\nu)^{1/2} = f(h\nu)$ in the photon energy range of 1.8-2.6 eV and $(\alpha h\nu)^2 = g(h\nu)$ in the photon energy range of 2.6-3.5 eV are linear function. This linearity indicates the existence of the allowed indirect and direct transitions. Values of E_g^{opt} and the constant A for the as-deposited In_2S_3 films are given in table 1.

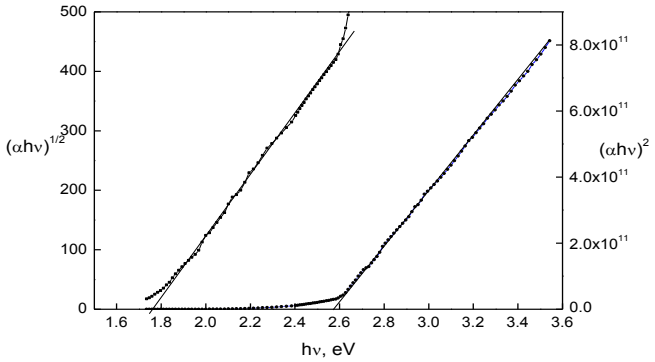

Fig.(5) Dependence of $(⍟h⍟)^{1/2}$ and $(⍟h⍟)^2$ on photon energy h⍟ for as-deposited In_2S_3 films.

Table (1)

Values of direct and indirect optical energy gap (E_g) and the constant A for as-deposited In_2S_3 films

Direct transitions		Indirect transitions	
E_g, eV	A	E_g, eV	A
2.55	8.73×10^5	1.77	2.68×10^5

Mathew et al. [11] found from absorption measurements for spray pyrolysis In_2S_3 film of thickness 0.25 ◎m that optical transitions are direct with optical energy gap of 2.57 eV. Bhira et al. [15] studied optical properties of In_2S_3 film of thickness 1.5 ◎m deposited onto pyrex glass substrates by spray pyrolysis technique. They found that optical transitions are direct with optical energy gap of 2.08 eV which is close to that value for bulk material[34]. Benchouk et al. [16] prepared In_2S_3 films by annealing indium thin films at different temperatures under sulfur pressure. They found from optical measurements a direct and indirect transitions with optical energy gap depending on the annealing temperature. Rajesh et al. [19] studied optical properties of In_2S_3 films of different thicknesses deposited onto ITO coated glass substrates by spin coating technique. They found that optical transitions are direct with optical energy gap of increased from 2.58 to 2.75 eV as the film thickness decreases from 550 to 200 nm. Revathi et al [20] prepared bulk In_2S_3 by simple solid state reaction. They found that optical transitions are direct with optical energy gap of 2.2 eV. Sterner et al. [22] prepared In_2S_3 films by atomic layer deposition. They found that optical transitions are direct with optical energy gap increases slightly with film thickness with average value of 2.08 eV. Allsop et al [35]prepared In_2S_3 films by spray ion layer gas reaction. They found that optical transitions are indirect with optical energy gap of 2.2 eV. Asikainen et al.[36] prepared polycrystalline◎◎-In_2S_3 films by atomic layer epitaxy and found that it has optical energy gap of 2.3 eV.

3-4 EFFECT OF ANNEALING

To illustrate the effect of annealing on the optical constants and optical energy gap of In_2S_3 films, we applied the annealing process as explained in section 2. Fig.(6) shows the dependence of transmittance at λ = 500 nm in the strong absorption region on the period of annealing at different temperatures from 323 K up to 573 K for a film of thickness 210 nm as a representative example. No distinguishable changes in transmittance were observed for films annealed at 323 and 373 K in comparison with transmittance carried out for as-deposited films. However, It is clear from the figure that transmittance increases with the increase of period of annealing at different temperatures less than or equal 523 K up to 4 h, then the transmittance becomes constant indicating the stability of the structure of the annealed films. For In_2S_3 films annealed at 573 K, the stability was obtained after annealing for 2 h only. The same results were obtained In_2S_3 films of different thicknesses.

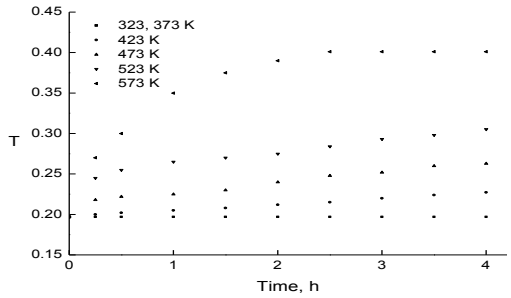

Fig.(6) Dependence of transmittance (T) at 500 nm on the time of annealing for In_2S_3 films annealed at different temperatures.

Fig.(7) shows the spectral distribution of transmittance and reflectance for In_2S_3 films annealed at different temperatures in the whole studied spectral range. Using the same procedure, the optical constants n, k were determined.

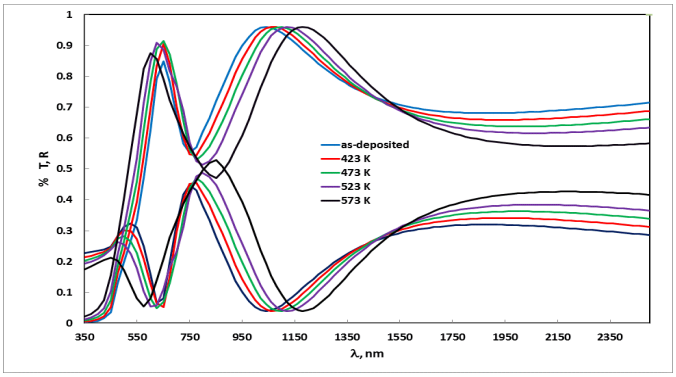

Fig.(7) The spectral distribution of transmittance (T) and reflectance (R) for In_2S_3 films annealed at different temperatures.

Fig.(8a,b) shows the spectral distribution of refractive index (n) and absorption index (k) for the annealed films with that of the as-deposited In_2S_3 films for comparison.

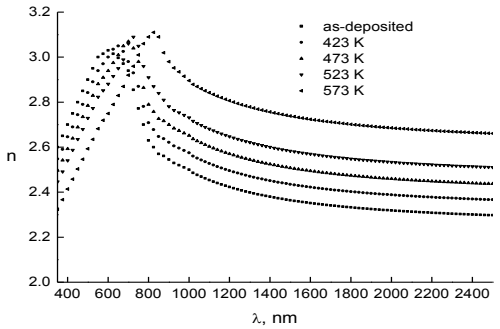

Fig.(8a) The spectral distribution of refractive index (n) for In_2S_3 films annealed at different temperatures.

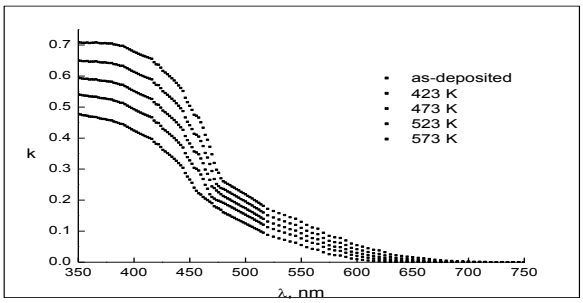

Fig.(8b) The spectral distribution of absorption index (k) for In_2S_3 films annealed at different temperatures.

The refractive index dispersion in semiconductors has been analyzed using the concept of the single-oscillator model. In this concept the energy parameters, single-oscillator energy (E_o) and dispersion energy (E_d) are introduced and the refractive index n at any photon energy h◎ is expressed by the Wemple–DiDomenico relationship[37]:

$$n^2-1 = E_o E_d /(E^2_o – (h\nu)^2) \quad (8)$$

The physical meaning of E_o is that it stimulates all the electronic excitation involved and takes values near the main peak of the imaginary part of the dielectric constant spectrum, while E_d is related to the average strength of the optical transitions. It is shown by earlier workers [38, 39] that: (i) E_d is independent of the absorption threshold (band gap), within experimental error (ii) E_d is independent of the lattice constant, within experimental error; and (iii) E_o is related to the lowest direct gap. In practice the dispersion parameters E_o and E_d are obtained using a simple plot of $(n^2 - 1)^{-1}$ against $(h\nu)^2$ as shown in Fig (9). It is observed that the plots are linear over the energy range from 0.22 eV^2 to approximately 1.8 eV^2. The refractive index n(0) at zero photon energy, which is defined by the high frequency dielectric constant ε_∞, can be deduced from the dispersion relationship by extrapolation of the linear part as in Fig(9). Values of E_o, E_d and ε_∞ are calculated and tabulated in Table (2).

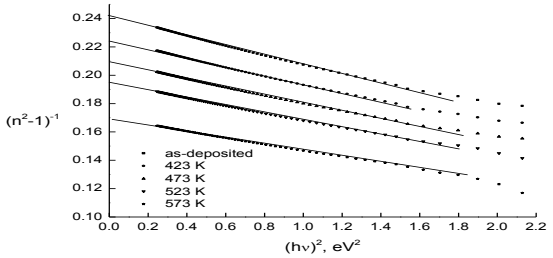

Fig.(9) Plots of $(n^2 - 1)^{-1}$ against $(h\nu)^2$ for In_2S_3 films annealed at different temperatures.

Table (2)

Values of single-oscillator energy (E_o), dispersion energy (E_d) and high frequency dielectric constant (ε_∞) for as-deposited and annealed In_2S_3 films

parameter	E_o, eV	E_d, eV	ε_∞
As-deposited films	2.76	11.11	5.12
Annealed at 423 K	2.74	12.17	5.44
Annealed at 473 K	2.72	12.94	5.78
Annealed at 523 K	2.70	13.98	6.13
Annealed at 573 K	2.64	16.38	7.21

The presentation of $(\alpha h\nu)^{1/2} = f(h\nu)$ in the photon energy range of 1.8-2.6 eV and $(\alpha h\nu)^{1/2} = f(h\nu)$ in the photon energy range of 2.6-3.5 eV are shown in Fig. (10) for the annealed In_2S_3 films at different temperatures . It is clear from the figure that the relations are linear. This linearity confirmed the existence of the allowed indirect and direct transitions for the annealed films as in case of as-deposited films. It is clear from the figure that absorption edge was shifted to higher photon energy. Values of E_g^{opt} and the constant A for the annealed In_2S_3 films are given in Table 1.

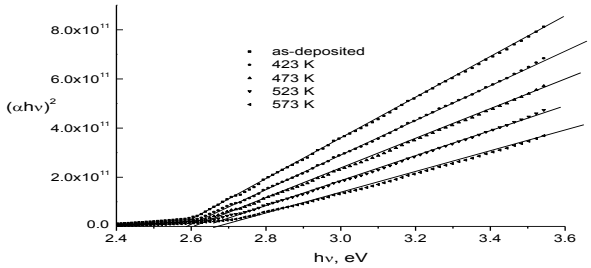

Fig.(10a) Dependence of $(◎h◎)^2$ on photon energy h◎ for In_2S_3 films annealed at different temperatures.

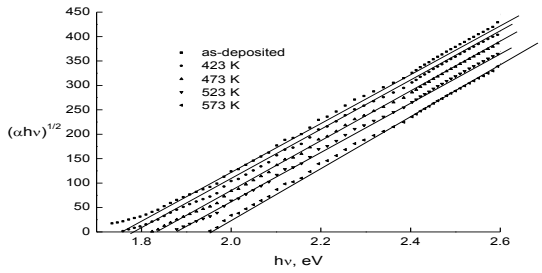

Fig.(10b) Dependence of $(\alpha h\nu)^{1/2}$ on photon energy hν for In_2S_3 films annealed at different temperatures.

From the table it is observed that allowed direct and indirect optical energy gap increases with the increase of annealing temperature, but the absorption coefficient decreases, which can be attributed to the low transitions probability of the carriers [39] across the corresponding large gap .

Table (3)

Values of direct and indirect optical energy gap (E_g) and the constant A for as-deposited and annealed In_2S_3 films

parameter	Direct transitions		Indirect transitions	
	E_g, eV	A	E_g, eV	A
As-deposited films	2.55	$8.73x10^5$	1.77	$2.68x10^5$
Annealed at 423 K	2.58	$8.45x10^5$	1.80	$2.62x10^5$
Annealed at 473 K	2.61	$7.75x10^5$	1.85	$2.58x10^5$
Annealed at 523 K	2.63	$7.25x10^5$	1.89	$2.53x10^5$
Annealed at 573 K	2.67	$6.32x10^5$	1.95	$2.50x10^5$

CONCLUSION

In_2S_3 films have been prepared by thermal evaporation technique. X-ray diffraction analysis for the as-deposited In_2S_3 films showed that they have amorphous structure. On annealing at 573 K films have a ◎- phase tetragonal polycrystalline structure. The optical constants n and k of the as-deposited and annealed films are practically independent on the film thickness in the range 210–470 nm. Analysis of optical constants yields some important constants such as single-oscillator energy (E_o) and dispersion energy (E_d). The optical absorption measurements indicate that the absorption is due to allowed indirect and direct for the as-deposited and annealed films. Annealing In_2S_3 films showed an increase in both indirect and direct energy gap. The obtained data confirmed that annealed In_2S_3 films can be used as a buffer layer for photovoltaic applications.

REFERENCES

1- K. Kambas and J. Spyridelis, Mat. Res. Bull. 13(1978)653.
2- C. Julien, M. Eddrief, K. Kambas and K. Nalkanski, Thin Film Films 137 (1986) 27.
3- A.E.Bekheet, J. Electronic Materials 17(2008) 540
4- M.A.Afifi, A.E.Bekheet, H.T.El-Shair and I.T.Zedan, Physica B 325 (c) p. 308 (2002).
5- A.E.Bekheet, European Physical Journal (Applied Physics) 16 (3) (2001) p. 187.
6- M.A.Afifi, E.Abd El-Wahabb, A.E.Bekheet and H.E.Atyia, Acta Physica Polonica A 98 (4) (2000) p. 401
7- N.A.Hegab, A.E.Bekheet ,M.A.Afifi and A.E.El-Shazly. Applied Physics A Vol. 66(1998) 235 -240.
8- C.S. Yoon, K.H. Park, D.T. Kim, T.Y. Park, M.S. Jin, S.K. Oh, and W.T. Kim, J. Phys. Chem. Solids 62(2001)1131.
9- S.M. Souza, C.E.M. Campos, J.C. de Lima, T.A. Grandi, and P.S. Pizani, Solid State Commun. 139, 70 (2006).
10- M.R. Asabe, P.A. Chate, S.D. Delekar, K.M. Garadkar, I.S. Mulla, P.P. Hankare, J. Phys. & Chem. Sol. 69 (2008) 249.
11- Meril Mathew , Manju Gopinath , C. Sudha Kartha , K. P.Vijayakumar ,Y. Kashiwaba , T. Abe, Solar Energy 84 (2010) 888.
12- Teny Theresa John, Meril Mathew, C. Sudha Kartha, K. P. Vijayakumar, T. Abe, Y. Kashiwaba, Sol. Energy. Mat. Sol. Cells, 89(2005)27.
13- N. Barreau, Solar Energy 83(2009)363.
14- Susanne Siebentritt, Solar Energy 77(2004)767.
15- L. Bhira, H. Essaidi, S. Belgacem, G. Couturier, J. Salardenne, N. Barreaux, J.C. Bernede, Phys. Stat. Sol (a). 181 (2000)427.
16- K. Benchouk, J. Ouerfelli, M. Saadoun, A. Siyoucef, Physics Procedia 2 (2009) 971.
17- N. Naghavi, S. Spiering, M. Powalla, B. Cavana, D. Lincot, Prog. Photovolt. Res. Appl. 11(2003)437.
18- Xuebo Cao, Li Gu, Lanjian Zhuge, Wenhu Qian, Cui Zhao, Xianmei Lan, Wenjun Sheng, Dan Yao, Colloids and Surfaces A: Physicochem. Eng. Aspects 297 (2007) 183.
19- M.R. Rajesh Menon, M.V.Maheshkumar, K.Sreekumar, C.Sudha Kartha, K.P.Vijayakumar, Solar Energy Materials & Solar Cells 94 (2010) 2212.
20- N. Revathi, P. Prathap and K.T. Ramakrishna Reddy, Energy Procedia 2 (2010) 195.
21- M.M. El-Nahass, B.A. Khalifa, H.S. Soliman, M.A.M. Seyam, Thin Solid Films 515(2006)1796.
22- J. Sterner, J. Malmstrom and L. Stolt, Prog. Photovolt: Res. Appl. 13(2005)179.
23- T. Asikainen, M. Ritala, M. Leskelä, Applied Surface Science 82-83(1994)122.
24- J. Herrero and J. Ortega, Solar Energy Materials 17(1988)357.
25- W. Rehwald and G. Harbeke, Journal of Physics and Chemistry of Solids 26(1965)1309.
26- R. Swanepoel, J. Phys. E: Sci. Instrum. 16(1983)
27- L. Ohlidal, K. Kavratil and E. Schmidt, Appl. Phys. E9, 1002 (1976).
28- L. Ohlidal and K. Kavratil, Thin Solid Films 150, 181 (1988).
29- Dp. Arndt, Appl. Opt. 23, 3571 (1984).
30- O. S. Heavns, Physics of Thin Films, Vol. 2, eds. G. Hass and R. Thus (Academic,New York, 1964), p. 193.
31- H. M. Liddel, Computer-aided Techniques for the Design of Multilayer Filter (Hilher,Bristol, 1981), p. 118.
32- J.Strong, Concepts of Classical Optics, Freeman, San Francisco, (1985).
33- A. Cavaleiro, C. Louro, Vacuum 64(2002)211.
34- W. Rehwald and G.Harbeke, J. Phys. Chem. Solids 26, 1309(1965).
35- N.A. Allsop , A. Schönmann, A. Belaidi, H.-J. Muffler, B. Mertesacker, W. Bohne, E. Strub, J. Röhrich, M.C. Lux-Steiner, and Ch.-H. Fischer, Thin Solid Films 513(2006)52.
36- T. Asikainen, M. Ritala and M. Leskelä, Applied Surface Science 82(1994)122
37- S.H. Wemple, M. DiDomenico, Phys. Rev. B 3(1971)1338.
38- E- T. Toyoda, J. Appl. Phys. 63 (1988) 5166.
39- B. Esser, D. Sprenger, Phys. Stat. Sol. B 94(1979)583.